

Third-Order Elastic Constants of Magnesium. I. Experimental*

E. R. Naimon[†]

*Department of Physics and Materials Research Laboratory,
University of Illinois, Urbana, Illinois 61801*

(Received 27 May 1971)

The complete set of ten third-order elastic constants of magnesium has been determined from measurements of the hydrostatic-pressure and uniaxial-compression derivatives of natural sound velocities using an ultrasonic pulse-superposition technique. The specimen was neutron irradiated with an integrated exposure of 2×10^{18} (fast) neutrons per cm^2 to suppress dislocation effects. The results are $c_{111} = -6.63$, $c_{112} = -1.78$, $c_{113} = +0.30$, $c_{222} = -8.64$, $c_{123} = -0.76$, $c_{133} = -0.86$, $c_{333} = -7.26$, $c_{144} = -0.30$, $c_{155} = -0.58$, and $c_{344} = -1.93$ in units of $10^{12} \text{ dyn cm}^{-2}$.

I. INTRODUCTION

The second-order elastic constants of magnesium have already been measured.¹⁻³ In addition, the hydrostatic-pressure derivatives of the second-order constants have been reported.⁴ This information, however, is not sufficient to determine the complete set of third-order constants. There are five second-order and ten⁵ third-order constants for crystals having the hcp structure. Thus the hydrostatic-pressure derivatives of the second-order constants give only five experimental numbers which are related to the ten third-order elastic constants. The present work is concerned with measurements to determine the complete set of third-order elastic constants of magnesium.

At the time this work was begun, there had been no third-order constants reported for any hcp metal. Recently, however, Swartz and Elbaum⁶ have measured the complete set of third-order elastic constants of zinc; they did not present any theory to account for their results. The hydrostatic-pressure derivatives of the second-order constants of the hcp metals Be,⁷ Cd,⁸ and Zr,⁹ have also been reported; as mentioned above, this information is insufficient to determine a complete set of third-order constants.

The additional information needed to experimentally determine a complete set of third-order elastic constants can be obtained by measuring the change of the second-order constants when only one crystalline axis is stressed at a time. Since second-order elastic constants are determined from measurements of the velocity of sound in a crystal, the third-order constants are then simply related to the change in sound velocity due to an applied homogeneous stress, such as hydrostatic pressure or uniaxial compression.

Unfortunately, uniaxial compression of metal crystals is likely to introduce dislocation motion, and it is well known that dislocations affect the measured sound velocity. It is possible to pin down

existing dislocations by neutron irradiating the metal sample. The stress level must then be kept low enough to prevent breakaway of dislocations from the pinning points. Stresses on the order of 10 bar appear to be sufficiently low to suppress dislocation effects. With such low stresses, the typical sound velocity changes are 10–100 ppm. Detection of such small velocity changes requires an extremely sensitive electronic system. A system capable of measuring relative velocity changes as small as 10^{-8} has recently been developed by Holder¹⁰ and was used in the present work.

The experimental determination of the complete set of ten third-order elastic constants will be presented in Sec. II, after which a discussion will follow in Sec. III.

II. EXPERIMENTAL PROCEDURE AND RESULTS

The single crystal of magnesium used throughout the experiment was obtained from Semi-Elements Inc., Saxonburg, Pa. The dimensions of the sample were approximately $18 \times 19 \times 20$ mm. The crystal was oriented with faces perpendicular to the $[1\bar{2}10]$, $[10\bar{1}0]$, and $[0001]$ directions, hereafter referred to as the a , b , and c axes, respectively. Laue backreflection photographs showed the orientations to be better than 1° . A spectral analysis provided with the sample claimed a composition of 99.95+% pure magnesium. The crystal was polished until opposite faces were flat and parallel to 200 ppm.

The second-order elastic constants were measured by the pulse-echo-overlap method of Papadakis;¹¹ 10-MHz quartz transducers were attached to the crystal with phenyl salicylate (salol). The transit times could be obtained to better than 2 nsec. By attaching a dummy transducer to the far end of the specimen, a transit time correction of 100 nsec/echo was determined for both longitudinal and shear waves. For purposes of comparison with the results of other investigators, a density of 1.738 g cm^{-3} was used. This made it possible to

TABLE I. The adiabatic second-order elastic constants of Mg at 25°C. The results of the other investigators were normalized to a density of 1.738 g cm⁻³ by Eros and Smith. Entries are in units of 10¹² dyn cm⁻².

<i>c</i>	This experiment	Eros and Smith	Long and Smith ^a	Slutsky and Garland ^b
<i>c</i> ₁₁	0.5918 ± 0.0008	0.5928	0.5969	0.5905
<i>c</i> ₃₃	0.6147 ± 0.0007	0.6135	0.616	0.6125
<i>c</i> ₆₆ = ½(<i>c</i> ₁₁ - <i>c</i> ₁₂)	0.1675 ± 0.0002	0.1669	0.1674	0.1680
<i>c</i> ₄₄	0.1634 ± 0.0006	0.1632	0.1638	0.1632
<i>c</i> ₁₃	...	0.2157	0.217	0.2130
<i>c</i> ₁₂	0.2568 ± 0.0009	0.2590	0.2622	0.2545

^aReference 2.

^bReference 3.

use the tabulated data of Eros and Smith¹ directly.

The constants *c*₁₁ and *c*₃₃ were determined from the propagation of longitudinal waves in the basal plane and along the *c* axis, respectively. The constant *c*₆₆ = ½(*c*₁₁ - *c*₁₂) was found from a shear wave propagated along the *a* (or *b*) axis and polarized along the *b* (or *a*) axis. The constant *c*₄₄ was determined from the shear wave propagated along the *c* axis, and from the shear wave propagated along the *a* or *b* axis and polarized along the *c* axis. We were not able to determine the constant *c*₁₃ due to the orientation of our crystal. We could only propagate waves parallel and perpendicular to the *c* axis, and *c*₁₃ can only be found by propagation at some other angle to the *c* axis. Throughout our work we will use the experimental value of *c*₁₃ determined by Eros and Smith.

Our results for the adiabatic second-order elastic constants are presented in Table I and compared with the values found by other investigators. Our results in every case fall within the range of their values. The errors presented are estimated from the uncertainties in the measured transit times and lengths.

After obtaining the second-order elastic constants, the magnesium crystal was neutron irradiated to suppress dislocation effects. The irradiation was performed at the reactor lab of the University of Illinois; the integrated exposure was approximately 2 × 10¹⁸ (fast) neutrons/cm².

We have used the pulse-superposition^{12,13} method with the improved detection system developed by Holder to measure the stress derivatives of the sound velocities. As in other velocity systems, the directly measured quantity is the relative change in frequency. This change is exactly the relative change of the natural velocity $w = 2L_0/t$, where *L*₀ is the unstressed path length and *t* is the round-trip transit time.

Before doing the stress experiments, we measured the temperature derivatives of the natural sound velocities. Then, for the stress experiments, we were able to normalize all the velocities to a standard temperature (22.000°C). The temperature was measured with Chromel-advance ther-

mocouples and could be determined to a millidegree.

The temperature derivatives were determined over the range 5–15°C. For these experiments the temperature was controlled by placing the specimen in a furnace which was surrounded by an ice bath. The temperature could be changed by adjusting the furnace-coil current. The temperature derivatives of the natural sound velocities are presented in Table II. The indicated errors represent the range of several measurements for each mode.

By considering the second-order elastic constants *c* to be functions of temperature *T* and pressure *P*, it can be shown that

$$\frac{\partial}{\partial T} (\ln c)_P = -\beta + 2\alpha_L + 2\frac{\partial}{\partial T} (\ln w)_P. \quad (1)$$

Here β is the volume thermal expansion coefficient and α_L is the coefficient of linear thermal expansion of the propagation axis. For magnesium, $\alpha_{||\text{ to }c} = 0.265$, $\alpha_{\perp\text{ to }c} = 0.251$, and $\beta = 2\alpha_{\perp} + \alpha_{||} = 0.767$ ¹⁴ in units of 10⁻⁴°C⁻¹. We have calculated $(\partial/\partial T)(\ln c)_P$ for the different modes and, in Table II, compared our values with those of Slutsky and Garland.³

Their results are in tabular form, and we have calculated the derivatives from their room-temperature values. Our values are expected to be more accurate at room temperature, since we measured the velocities at ten points over a 10° interval. Slutsky and Garland measured velocities over the temperature range of 4.2–300°K in 20° intervals.

We then proceeded to measure the hydrostatic-

TABLE II. The logarithmic temperature derivatives on the natural velocities and of the second-order elastic constants of Mg. Entries are in units of 10⁻⁴°C⁻¹.

<i>c</i>	$\frac{\partial}{\partial T} (\ln w)_P$	This experiment	Slutsky and Garland
<i>c</i> ₁₁	-1.467 ± 0.012	-3.20 ± 0.02	-2.86
<i>c</i> ₃₃	-1.49 ± 0.01	-3.22 ± 0.02	-3.25
<i>c</i> ₆₆ = ½(<i>c</i> ₁₁ - <i>c</i> ₁₂)	-2.43 ± 0.02	-5.12 ± 0.05	-4.44
<i>c</i> ₄₄ (along <i>c</i> axis)	-2.38 ± 0.01	-5.01 ± 0.02	-5.79
<i>c</i> ₄₄ (basal plane)	-2.375 ± 0.010		

TABLE III. The sound-velocity stress experiments.

Expt. No.	Propagation axis	Polarization axis	Stress axis	<i>c</i>
1	<i>c</i>	<i>b</i>	hydro.	<i>c</i> ₄₄
2	<i>b</i>	<i>a</i>	hydro.	<i>c</i> ₆₆
3	<i>b</i>	<i>b</i>	hydro.	<i>c</i> ₁₁
4	<i>c</i>	<i>c</i>	hydro.	<i>c</i> ₃₃
5	<i>c</i>	<i>c</i>	<i>b</i>	<i>c</i> ₃₃
6	<i>b</i>	<i>b</i>	<i>c</i>	<i>c</i> ₁₁
7	<i>b</i>	<i>b</i>	<i>a</i>	<i>c</i> ₁₁
8	<i>a</i>	<i>a</i>	<i>b</i>	<i>c</i> ₁₁
9	<i>b</i>	<i>a</i>	<i>c</i>	<i>c</i> ₆₆
10	<i>b</i>	<i>a</i>	<i>a</i>	<i>c</i> ₆₆
11	<i>a</i>	<i>b</i>	<i>b</i>	<i>c</i> ₆₆
12	<i>b</i>	<i>c</i>	<i>c</i>	<i>c</i> ₄₄
13	<i>b</i>	<i>c</i>	<i>a</i>	<i>c</i> ₄₄
14	<i>c</i>	<i>b</i>	<i>b</i>	<i>c</i> ₄₄

$a = [1\bar{2}10], \quad b = [10\bar{1}0], \quad c = [0001]$

pressure and uniaxial-stress derivatives of the natural sound velocities. Hydrostatic pressure was obtained from a nitrogen gas tank and was measured by a Heise bourdon gauge. The pressure vessel contained a heater coil to keep temperature corrections to a minimum. The stress range for hydrostatic experiments was approximately 0–80 kg cm⁻². A Tinius Olsen universal testing machine, accurate to better than 1%, was used to apply uniaxial compression. The crystal was placed between indium shims when stressed, and the stress was applied through a ball joint to promote uniform compression. Here the stress range was kept below 20 kg cm⁻², except for the *c*₄₄ modes, for which the stress never exceeded 6 kg cm⁻².

For a hcp crystal oriented with faces perpendicular to the *a*, *b*, and *c* axes, there are four hydrostatic and ten uniaxial experiments to determine the ten third-order elastic constants. These experiments are listed in Table III. For each experiment the directly measured quantity is $(\partial/\partial P)(\ln w)_{T,P=0}$. It is easily shown that

$$\frac{\partial}{\partial P} (\rho_0 w^2)_{T,P=0} = 2c \frac{\partial}{\partial P} (\ln w)_{T,P=0}, \quad (2)$$

where *c* is the appropriate second-order elastic constant and ρ_0 is the density of the unstressed material. The relations between the measured quantities $(\partial/\partial P)(\rho_0 w^2)_{T,P=0}$ and the second- and third-order elastic constants have been found by Thurston and Brugger^{15,16} and are summarized in Table IV.

The coefficients *s*_{*ij*} of the elastic constants in Table IV are the isothermal elastic compliances. They are related to the adiabatic compliances *s*_{*ij*}^{*S*} by¹⁷

$$s_{ij}^{(T)} = s_{ij}^S + T \alpha_i \alpha_j / \rho_0 c_P. \quad (3)$$

Here α_i and α_j are the linear thermal-expansion

coefficients, and *c*_{*P*} is the specific heat at constant pressure (0.245 cal g⁻¹ °C⁻¹ for Mg).¹⁴ The values of the isothermal compliances of Mg are given in Table IV.

The hydrostatic-pressure derivatives of the natural sound velocities were measured first, experiments 1–4 of Tables III and IV. The velocity change for a typical hydrostatic experiment is shown in Fig. 1. From the measured quantities $(\partial/\partial P) \times (\rho_0 w^2)_{T,P=0}$, we calculated the hydrostatic-pressure derivatives of the second-order elastic constants. It is easily shown that

$$\frac{\partial c}{\partial P} \Big|_{T,P=0} = \frac{\partial}{\partial P} (\rho_0 w^2)_{T,P=0} + c(K - 2K_L), \quad (4)$$

where *K* is the isothermal bulk compressibility and *K*_{*L*} is the isothermal linear compressibility of the propagation axis; the values of *K*₁ and *K*₃ are given in Table IV. The pressure derivatives of the elastic constants are compared in Table V to the values

TABLE IV. Relationships between the sound velocity stress derivatives and the elastic constants.

Expt. No.	$-\frac{\partial}{\partial P} (\rho_0 w^2)_{T,P=0}$
1	$2c_{44}K_1 + K_1(c_{144} + c_{155}) + K_3c_{344} + 1$
2	$2c_{66}K_1 + \frac{1}{2}K_1(c_{222} - c_{112}) + \frac{1}{2}K_3(c_{113} - c_{123}) + 1$
3	$2c_{11}K_1 + K_1(c_{111} + c_{112}) + K_3c_{113} + 1$
4	$2c_{33}K_3 + 2K_1c_{133} + K_3c_{333} + 1$
5	$2c_{33}s_{13} + (s_{11} + s_{12})c_{133} + s_{13}c_{333}$
6	$2c_{11}s_{13} + s_{13}(c_{111} + c_{112}) + s_{33}c_{113}$
7	$2c_{11}s_{12} + s_{12}c_{111} + s_{11}c_{112} + s_{13}c_{113}$
8	$2c_{11}s_{12} + s_{11}(c_{111} + c_{112}) + (s_{12} - s_{11})c_{222} + s_{13}c_{113}$
9	$2c_{66}s_{13} + \frac{1}{2}s_{13}(c_{222} - c_{112}) + \frac{1}{2}s_{33}(c_{113} - c_{123})$
10	$2c_{66}s_{11} + \frac{1}{2}(s_{11} - s_{12})c_{111} - \frac{1}{4}(s_{11} + s_{12})c_{112} + \frac{1}{4}(3s_{12} - s_{11})c_{222} + \frac{1}{2}s_{13}(c_{113} - c_{123})$
11	$2c_{66}s_{11} - \frac{1}{2}(s_{11} - s_{12})c_{111} - \frac{1}{4}(s_{11} + s_{12})c_{112} + \frac{1}{4}(3s_{11} - s_{12})c_{222} + \frac{1}{2}s_{13}(c_{113} - c_{123})$
12	$2c_{44}s_{33} + s_{13}(c_{144} + c_{155}) + s_{33}c_{344}$
13	$2c_{44}s_{13} + s_{11}c_{144} + s_{12}c_{155} + s_{13}c_{344}$
14	$2c_{44}s_{11} + s_{12}c_{144} + s_{11}c_{155} + s_{13}c_{344}$
	$s_{11} = s_{11}^T = 2.220 \times 10^{-12} \text{ cm}^2 \text{ dyn}^{-1}$
	$s_{33} = s_{33}^T = 1.992 \times 10^{-12} \text{ cm}^2 \text{ dyn}^{-1}$
	$s_{12} = s_{12}^T = -0.765 \times 10^{-12} \text{ cm}^2 \text{ dyn}^{-1}$
	$s_{13} = s_{13}^T = -0.493 \times 10^{-12} \text{ cm}^2 \text{ dyn}^{-1}$
	$K_1 = s_{11}^T + s_{12}^T + s_{13}^T = 0.962 \times 10^{-12} \text{ cm}^2 \text{ dyn}^{-1}$
	$K_3 = s_{33}^T + 2s_{13}^T = 1.006 \times 10^{-12} \text{ cm}^2 \text{ dyn}^{-1}$

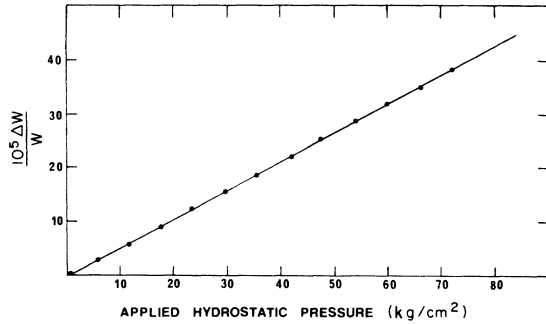


FIG. 1. Natural velocity change vs hydrostatic pressure for a c_{33} mode (experiment 4 of Tables III and IV).

found by Schmunk and Smith.⁴ The error indicated with our results represents the range of several measurements. It should be noted here that very good agreement exists despite the difference in the pressure ranges; our experiments never exceeded 80 bar, whereas Schmunk and Smith worked in the kilobar region. Similar type comparisons have not been as good for the metals Cu, Ag, Au,¹⁸ and Al,¹⁹ for which a two-specimen interferometric technique was used for the low-stress range.

We then performed the uniaxial experiments involving the c_{33} , c_{11} , and c_{66} modes, experiments 5–11 of Tables III and IV. A typical natural velocity change for a uniaxial-compression experiment is shown in Fig. 2. For convenience only, some of the experiments were begun with a stress applied; they could have been started with no stress. Before carrying out the experiments which involved c_{44} , experiments 12–14 of Tables III and IV, it was necessary to neutron irradiate the crystal once more; apparently the effects of the first irradiation had annealed out over a period of several months of handling. This was not observable in the other experiments since they are not dislocation sensitive. By a dislocation-sensitive experiment we mean one for which there is a component of shear stress in the slip plane. The primary slip plane of the hcp structure is the basal plane. Since we always compressed either parallel or perpendicular to the basal plane, the uniaxial stresses have no

TABLE V. The hydrostatic-pressure derivatives of the second-order elastic constants of Mg.

c	This expt.	Schmunk and Smith
	$\left(\frac{\partial c}{\partial P}\right)_{T, P=0}$	
c_{44}	1.60 ± 0.04	1.58
c_{66}	1.37 ± 0.02	1.36
c_{11}	6.23 ± 0.20	6.13
c_{33}	7.29 ± 0.03	7.22

shear components in the base. However, the c_{44} sound wave does have a shear-stress component in the basal plane. This means that experiments 1 and 12–14 of Table III are dislocation sensitive. That these modes were dislocation sensitive was borne out by the high attenuation of the propagating wave. For the second irradiation, the integrated exposure again was approximately 2×10^{18} (fast) neutrons per cm^2 .

We then performed the remaining uniaxial compression experiments; the stress level was kept extremely low, never exceeding 6 kg cm^{-2} . The results of the c_{44} experiments are less accurate than those of the other experiments for two reasons:

(a) The stress levels were much lower, resulting in smaller velocity changes, and (b) the ultrasonic attenuation was higher, resulting in a decrease in sensitivity. The natural velocity could only be determined to 2 ppm, whereas a part in 10^7 was easily attainable for the other experiments. The natural velocity change for a typical c_{44} uniaxial compression experiment is shown in Fig. 3.

The results for all the hydrostatic and uniaxial experiments are summarized in Table VI. The errors indicated represent the range of the measured values.

Salama and Alers²⁰ have suggested that agreement between hydrostatic and uniaxial data is a good indication that dislocation effects are not present. No dislocation motion should occur during hydrostatic-pressure experiments, so a comparison of the two sets of data should show whether uniaxial compression has introduced dislocation effects. We were able to make three such comparisons. The third-order constants c_{144} , c_{155} , and c_{344} were determined from the uniaxial data of experiments 12–14; the combination $[c_{144} + c_{155} + (K_3/K_1)c_{344}]$ was then calculated and compared to the hydrostatic value obtained from experiment 1. Then, from the uniaxial data of experiments 6–10, we determined the constants c_{111} , c_{112} , c_{113} , c_{222} , and c_{123} ; the

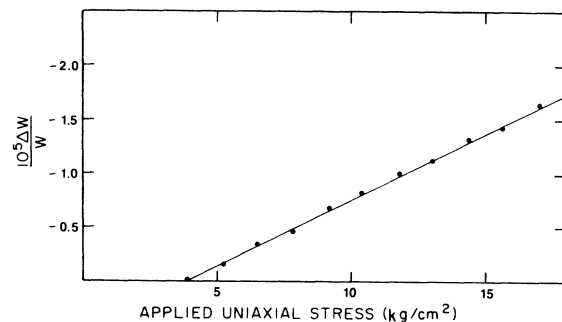


FIG. 2. Natural velocity change vs applied uniaxial stress for a c_{33} mode (experiment 5 of Tables III and IV). Experiment was begun with a 3.90-kg cm^{-2} stress applied to the specimen.

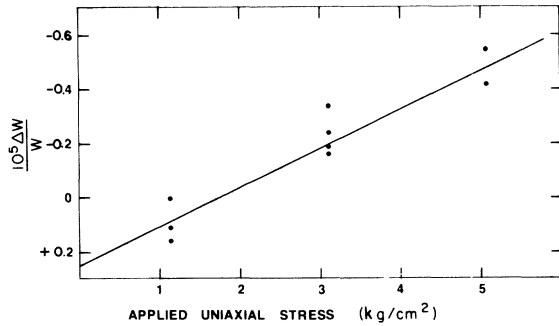


FIG. 3. Natural velocity change vs applied uniaxial stress for a c_{44} mode (experiment 13 of Tables III and IV).

combinations $[c_{111} + c_{112} + (K_3/K_1)c_{113}]$ and $[c_{222} - c_{112} + (K_3/K_1)(c_{113} - c_{123})]$ were calculated and compared to the values obtained from hydrostatic experiments 3 and 2, respectively. The comparisons are presented in Table VII. Our agreement in Table VII is sufficient to assume that dislocations have not contributed to the measured stress derivatives.

We should mention that experiment 11 was not included in calculating the values for Table VII. The results for this experiment are approximately 20% higher than those obtained from the other hydrostatic and uniaxial experiments, and thus were not included for the comparisons. We have no definite explanation for this disagreement. The results of experiment 11 are used, however, in the determination of the complete set of third-order elastic constants. The inclusion of this experiment does not affect the values of the third-order constants; it does, however, increase the resulting standard deviations.

The hydrostatic and uniaxial data were then combined to obtain the third-order elastic constants. A least-squares program was used to determine the "best" values. The constants c_{133} and c_{333} were de-

TABLE VI. Experimental data and results for sound-velocity stress derivatives.

Expt. No.	c (10^{12} dyn cm $^{-2}$)	$\frac{\partial}{\partial T}(\ln v)_P$ (10^{-4} C $^{-1}$)	$\frac{\partial}{\partial P}(\ln v)_{T, P=0}$ (10^{-12} dyn $^{-1}$ cm 2)	$\frac{\partial}{\partial P}(\rho_0 v^2)_{T, P=0}$ (dimensionless)
1	0.1634	-2.38	4.44 ± 0.13	1.45 ± 0.04
2	0.1675	-2.43	3.60 ± 0.05	1.20 ± 0.02
3	0.5918	-1.467	4.76 ± 0.17	5.64 ± 0.20
4	0.6147	-1.49	5.46 ± 0.02	6.72 ± 0.03
5	0.6147	-1.49	-1.40 ± 0.15	-1.72 ± 0.18
6	0.5918	-1.467	-3.50 ± 0.06	-4.14 ± 0.07
7	0.5918	-1.467	-0.19 ± 0.02	-0.22 ± 0.02
8	0.5918	-1.467	-5.00 ± 0.03	-5.92 ± 0.03
9	0.1675	-2.43	-6.92 ± 0.21	-2.32 ± 0.07
10	0.1675	-2.43	-2.58 ± 0.02	-0.86 ± 0.01
11	0.1675	-2.43	16.32 ± 0.84	5.47 ± 0.28
12	0.1634	-2.375	8.63 ± 1.95	2.82 ± 0.64
13	0.1634	-2.375	-1.54 ± 0.36	-0.50 ± 0.12
14	0.1634	-2.38	-1.65 ± 0.44	-0.54 ± 0.14

TABLE VII. Comparison of hydrostatic and uniaxial data. Entries are in units of 10^{12} dyn cm $^{-2}$. Indicated errors in the hydrostatic results represent the range of several measurements for each mode. Indicated errors in the uniaxial results represent our confidence in the values.

Elastic const	Hydrostatic	Uniaxial
$c_{144} + c_{155} + (K_3/K_1)c_{344}$	-2.87 ± 0.04	-3.12 ± 0.70
$c_{111} + c_{112} + (K_3/K_1)c_{113}$	-8.08 ± 0.20	-8.47 ± 0.80
$c_{222} - c_{112} + (K_3/K_1)(c_{113} - c_{123})$	-5.25 ± 0.04	-6.17 ± 0.50

$$\frac{K_3}{K_1} = (s_{33}^T + 2s_{13}^T)/(s_{11}^T + s_{12}^T + s_{13}^T) = 1.046$$

termined from experiments 4 and 5; the constants c_{111} , c_{112} , c_{113} , c_{222} , and c_{123} were determined from experiments 2, 3, and 6–11; and the constants c_{144} , c_{155} , and c_{344} were determined from experiments 1 and 12–14. The only weighting done was for the c_{44} experiments, where we felt that the hydrostatic measurement (experiment 1) was three times more accurate than the uniaxial measurements (experiments 12–14). The complete set of third-order elastic constants is presented in Table VIII. The errors indicated are the standard deviations arising from the least-squares analysis and represent the consistency of the measurements.

III. DISCUSSION

It is of interest to see if the Cauchy relations are satisfied for the elastic constants of magnesium. These are simple relations that can be derived when the interactions between atoms are due to central forces and when each atom is at a center of symmetry. The Cauchy relations for the second-order elastic constants are $c_{13} = c_{44}$ and $c_{12} = c_{66}$; the third-order Cauchy relations are

$$c_{456} = c_{366} = c_{144} = c_{123}, \quad c_{166} = c_{112}, \quad (5)$$

$$c_{266} = c_{122}, \quad c_{155} = c_{113}, \quad c_{344} = c_{133}.$$

Many of these constants are not the tabulated values, but linear combinations of them. The relations⁵ and values are

$$c_{166} = \frac{1}{4}(3c_{222} - 2c_{111} - c_{112}) = -2.72,$$

$$c_{266} = \frac{1}{4}(2c_{111} - c_{222} - c_{112}) = -0.71,$$

$$c_{366} = \frac{1}{2}(c_{113} - c_{123}) = 0.53,$$

$$c_{456} = \frac{1}{2}(c_{155} - c_{144}) = -0.14,$$

$$c_{122} = c_{111} - c_{222} + c_{112} = 0.23,$$

in units of 10^{12} dyn cm $^{-2}$.

From the above values and those of Tables I and VIII, it can be seen that the Cauchy relations are not satisfied. There does not seem to be a trend toward the Cauchy relations becoming satisfied for higher-order elastic constants. This is in contrast to the results obtained for the noble metals¹⁸,

TABLE VIII. The third-order elastic constants of Mg at 22 °C. Entries are in units of 10^{12} dyn cm⁻².

c_{133}	$= -0.86 \pm 0.03$
c_{333}	$= -7.26 \pm 0.06$
c_{111}	$= -6.63 \pm 0.25$
c_{112}	$= -1.78 \pm 0.14$
c_{113}	$= +0.30 \pm 0.16$
c_{222}	$= -8.64 \pm 0.25$
c_{123}	$= -0.76 \pm 0.35$
c_{144}	$= -0.30 \pm 0.03$
c_{155}	$= -0.58 \pm 0.03$
c_{344}	$= -1.93 \pm 0.03$

there, however, the dominant contributions to the higher-order constants were central-force-type interactions and the atoms were at centers of sym-

metry.

In Paper II we see that a good account of both the second- and third-order elastic constants is provided by a pseudopotential calculation. The failure of the Cauchy relations is accounted for both by the noncentral character of the forces and the fact that the atoms are not at centers of symmetry.

ACKNOWLEDGMENTS

The author would like to express his gratitude to his thesis advisor, Professor A. V. Granato, for his encouragement and advice. He also wishes to thank Professor J. Holder for introducing him to the experimental techniques and E. R. Fuller, Jr., for his invaluable aid in performing the experiments.

*Research supported by the U. S. Atomic Energy Commission under Contract No. AT(11-1)-1198.

†Based on a thesis submitted in partial fulfillment of the requirements for the degree of Ph. D. at the University of Illinois, 1970.

¹S. Eros and C. S. Smith, *Acta Met.* **9**, 14 (1961).

²T. R. Long and C. S. Smith, *Acta Met.* **5**, 200 (1957).

³L. J. Slutsky and C. W. Garland, *Phys. Rev.* **107**, 972 (1957).

⁴R. E. Schmunk and C. S. Smith, *J. Phys. Chem. Solids* **9**, 100 (1959).

⁵K. Brugger, *J. Appl. Phys.* **36**, 759 (1965).

⁶K. Swartz and C. Elbaum, *Phys. Rev. B* **1**, 1512 (1970).

⁷D. J. Silversmith and B. L. Averbach, *Phys. Rev. B* **1**, 567 (1970).

⁸J. A. Corll, ONR Technical Report No. 6, 1962 (unpublished).

⁹E. S. Fisher, M. H. Manghni, and T. J. Sokolowski,

J. Appl. Phys. **41**, 2991 (1970).

¹⁰J. Holder, *Rev. Sci. Instr.* **41**, 1355 (1970).

¹¹E. P. Papadakis, *J. Acoust. Soc. Am.* **42**, 1045 (1967).

¹²H. J. McSkimin, *J. Acoust. Soc. Am.* **33**, 12 (1961).

¹³H. J. McSkimin and P. Andreatch, *J. Acoust. Soc. Am.* **34**, 609 (1962).

¹⁴*American Institute of Physics Handbook* (McGraw-Hill, New York, 1963).

¹⁵R. N. Thurston and K. Brugger, *Phys. Rev.* **133**, A1604 (1964).

¹⁶K. Brugger, *J. Appl. Phys.* **36**, 768 (1965).

¹⁷R. F. S. Hearmon, *Rev. Mod. Phys.* **18**, 409 (1946).

¹⁸Y. Hiki and A. V. Granato, *Phys. Rev.* **144**, 411 (1966).

¹⁹J. F. Thomas, Jr., *Phys. Rev.* **175**, 955 (1968).

²⁰K. Salama and G. A. Alers, *Phys. Rev.* **161**, 673 (1967).